

WAAS at 15

Todd Walter, *Stanford University*

Karl Shallberg, *Zeta Associates Incorporated*

Eric Altshuler, *Sequoia research Corporation*

William Wanner, *William J. Hughes FAA Technical Center*

Chris Harris, *FAA WAAS Engineering Team*

Robert Stimmler, *Raytheon Company*

Abstract

The Wide Area Augmentation System (WAAS) achieved Initial Operating Capability (IOC) in July 2003. At IOC, WAAS had 25 reference stations in the conterminous United States, Hawaii, Alaska and San Juan Puerto Rico, two master stations, and four uplink stations supporting two narrowband L1 only GEO satellites. Today, WAAS has 38 reference stations including four in Canada and five in Mexico, three master stations, and six uplink stations supporting three wide band L1/L5 GEO satellites. In addition to the architectural expansion, the FAA continued to evolve and maintain the algorithms, hardware and software. With WAAS now turning fifteen years of age, this paper takes stock of these modifications and details the improved service and integrity that has occurred since 2003.

Introduction

WAAS was the first Satellite Based Augmentation System (SBAS) to be developed when it became operational in July 2003. The goal of any SBAS is to provide precise navigation for aircraft down to 200 feet above the ground over the whole of a state's airspace [1]. The IOC version of WAAS did not quite fulfill that goal. Although it did provide coverage over most of the Conterminous United States (CONUS), it did not cover all of the airspace, nor did it provide service down to 200 feet. In the ensuing years WAAS has made many improvements to its service by expanding and upgrading its hardware and by making improvements to its software [2].

The modifications to WAAS since IOC have touched all aspects of the system from adding reference stations, improving the ionospheric algorithms, refreshing the hardware such as reference receivers and antennas, enhancing communications networks for increased capacity of L5 measurements, and integrating new L1/L5 GEO satellites. This paper presents the major system modifications over this timeframe and demonstrates the resulting service improvements. We believe this information to be valuable to other Satellite Based Augmentation System providers lending insight into the evolution and maintenance of a system as complex as WAAS.

Service improvements are demonstrated using both historical performance and the MatLab Algorithm Availability Simulation Tool (MAAST) to show WAAS availability [3]. MAAST was developed by Stanford and has been proven to accurately reflect availability of the WAAS system. Proposed modifications to WAAS were evaluated using MAAST to show the resulting WAAS service improvements over the past fifteen years and will continue to be used for upcoming planned improvements. WAAS modifications that did not result in performance improvements but were important for safety, continuity, and maintainability will also be discussed. Some of the more notable algorithms implemented in WAAS since IOC were the extreme storm detector and signal quality monitoring.

WAAS Architecture Overview

To provide a frame of reference for the following discussion, Figure 1 provides depiction of the overall architecture of WAAS. It has a geographically diverse network of WAAS Reference Stations (WRSs) each containing three parallel threads of equipment. These WAAS Reference Elements (WREs) each consist of a GPS antenna, a GPS receiver, a cesium clock, and a computer to format the data and send it to the WAAS Master Stations (WMSs). The data is sent along redundant dedicated communication lines to ensure timely arrival and to minimize transmission loss. Each WMS has a Corrections and Verification (C&V) subsystem that consists of two parts: a corrections processor (CP) and a safety processor (SP). The corrections and integrity bounds estimated at the WMSs are formatted into messages that are provided to Ground Uplink

Stations (GUSs) for transmission to Geostationary Earth Orbit (GEO) satellites. The GEOs downlink this data on the L1 frequency with a modulation similar to that used by GPS.

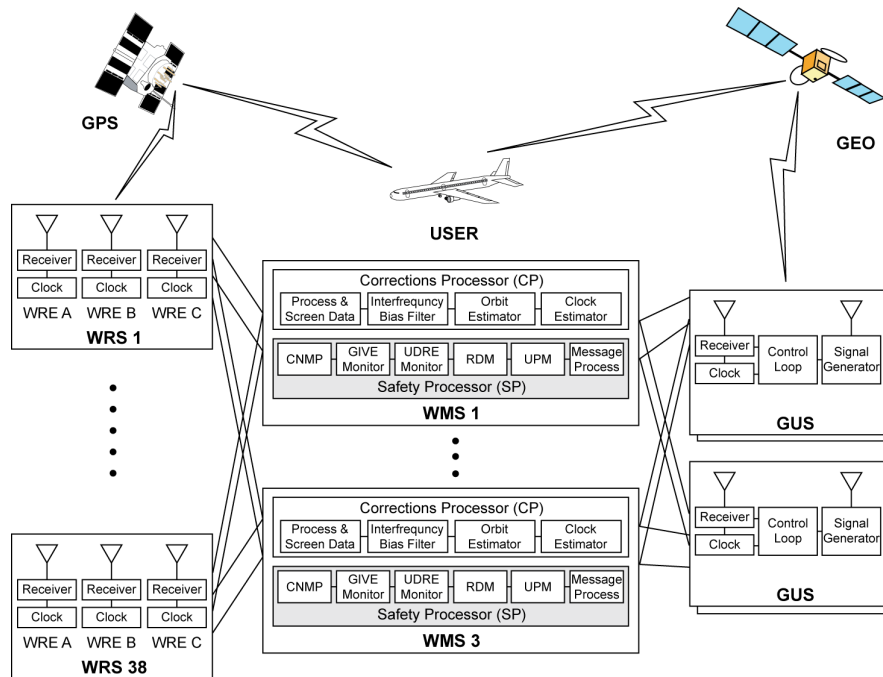


Figure 1. WAAS System Architecture

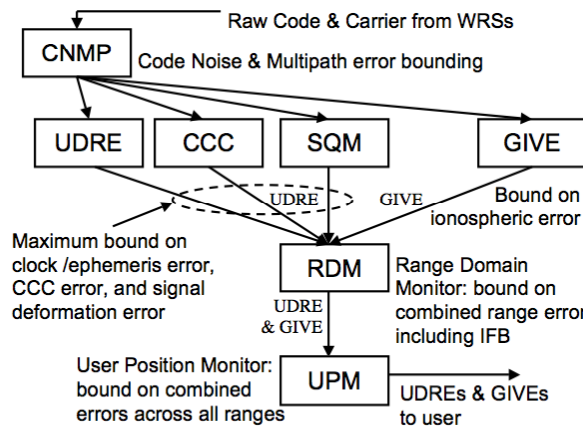


Figure 2. A schematic of the major integrity monitors.

The CP performs an initial screening of the data to identify and remove outliers. The resulting output is fed into a filter that estimates the receiver and satellite Inter-Frequency Biases (IFBs), and into filters that estimate the WRE clock offsets, the satellite orbital locations, and the satellite clock offsets. These are then passed along to the SP for evaluation. The SP is responsible for ensuring the safety of the WAAS output. It will decide what information will be sent to the user and to what level such information can be trusted. The SP performs its own independent data screening on the input WRE data. Its Code Noise and MultiPath (CNMP) monitor [4] performs data screening, carrier smoothing and produces a confidence bound for the remaining uncertainty on the smoothed pseudorange values. Figure 2 shows the SP monitoring algorithms and information flow. The User Differential Range Error (UDRE) monitor takes in the smoothed iono-free pseudoranges and bounds from the CNMP monitor and uses them to determine a confidence bound on the satellite clock and orbital correction errors from the CP. The Code Carrier Coherence (CCC) monitor and the Signal Quality Monitor (SQM) use inputs

from CNMP to determine whether or not the UDRE bound is sufficiently large to protect against potential code-carrier divergence and/or signal deformations respectively.

In parallel, the Grid Ionospheric Vertical Error (GIVE) monitor takes in the smoothed ionospheric delay estimates and bounds from the CNMP monitor as well as the IFB estimates from the CP to estimate the ionospheric delays and confidence bounds for a set of Ionospheric Grid Points (IGPs) defined to exist 350 km above the WAAS service area [5]. The user is able to interpolate between these IGPs to determine an ionospheric delay correction and corresponding confidence bound for each of their satellite measurements. The Range Domain Monitor (RDM) then evaluates all of the corrections and confidence bounds. The RDM uses smoothed L1 measurements and bounds from the CNMP monitor to determine whether corrections and bounds from the prior monitors combine as expected to bound the fully corrected single frequency measurements. If there is a problem, the RDM may increase the corresponding UDRE and GIVE values or it may flag the satellite as unsafe to use. All of this information is then passed to the User Position Monitor (UPM), which evaluates whether all the corrected position errors at each WRE are properly bounded. Like the RDM it too has the ability to increase the broadcast bounds or set a satellite as unusable. Finally, the corrections, UDREs and GIVES are broadcast to the user in a sequence of messages.

The remainder of this paper describes WAAS expansion, significant equipment refresh and maintenance activities, performance and integrity enhancements, and an overview on aviation adoption of the WAAS service.

System Expansion

The WAAS architectural expansion since IOC focused on improving performance, enhancing robustness, or addressing obsolescence. The addition of both a third C&V and a third GEO increased the robustness of the system by providing additional redundancy. The addition of Alaska, Canada and Mexico WRSs improved performance by providing better coverage in CONUS and Alaska and also expanding coverage to Canada and Mexico. The replacement of the initial GEOs with newer GEOs both improved performance and dealt with obsolescence of aging satellites. The expansion of the terrestrial communications infrastructure was driven by adding new sites to the system, dealing with obsolescence and adding bandwidth in preparation for future dual frequency capability. The paragraphs that follow will provide more detail and rationale for the architectural expansion.

Third C&V

Shortly after IOC the FAA planned for a series of enhancements that would be implemented in the system over the next several years. The FAA has a stringent requirement that the Signal in Space (SIS) must be maintained regardless of any upgrade or maintenance activity being performed on the system. WAAS at IOC only had two C&Vs. For earlier upgrades to the system, as one C&V was shut down for the upgrade, only one C&V was left running. With only one C&V running during these activities WAAS was vulnerable to a loss of SIS if the only remaining C&V failed. The mitigation for this risk was to add a third C&V to the system. With a third C&V, as one of the C&Vs is being upgraded there are still two other C&Vs running and providing the needed redundancy to maintain the SIS.

Expansion of WRSs

One widely recognized enhancement for WAAS has been the addition of reference stations. Although WAAS IOC did provide coverage over most of CONUS, it did not cover all of the airspace, nor did it provide service down to 200 feet. The primary goal of adding WRSs to the system is to maximize coverage in the area and increase availability of those areas that did not already meet 100% availability. The first part of this methodology for choosing new sites was to choose critical points. These critical points are the points of the service volume where improvements in availability are focused. The second part of this analysis involved running combinations of sites to assess their benefits as they act upon each other. The combinations of sites are chosen from the list of single sites that perform the best at each critical point. These combinations are run with the full user grid to measure overall coverage. A list of possible sites was proposed based on accessibility and feasibility of a location. These sites are limited to cities with proper infrastructure or places where proper infrastructure can be constructed to support the WRS. The end result was adding thirteen sites. Four new sites were added to Alaska, four sites were placed in Canada and five sites were placed in Mexico. Refer to Figure 3 for the location of the original IOC WRSs (red circles), four added Alaska WRSs (orange circles) and nine added international WRSs (purple diamonds).

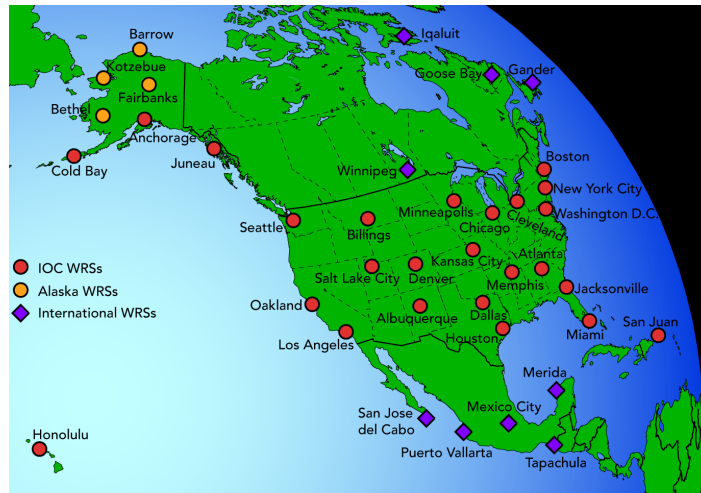


Figure 3. The location of the WAAS reference stations

Third GEO

Two GEOs are sufficient to provide the needed redundancy to maintain SIS for the WAAS system. The reason for adding a third GEO was to mitigate the lengthy time that was needed to deploy another GEO in the event that one of the two WAAS GEOs failed. The schedule to deploy a replacement GEO can take up to three years. During that three-year period, WAAS would be exposed to the risk of a loss of SIS if the remaining GEO failed, or if the ground uplink stations failed to provide a SIS to that GEO. WAAS leased the Inmarsat American Region (AMR) satellite from 2010 through 2017 to provide this third GEO signal.

GEO Replacements

Since IOC, the Inmarsat Atlantic Ocean Region (AOR) and Pacific Ocean Region (POR) GEOs have been replaced with the Intelsat Galaxy XV (internally labeled as CRW) and the Telesat Canada Anik F1R (labeled as CRE) satellites. One of the benefits of transitioning to the CRW and CRE GEOs was that they provided a better GPS like L1 ranging signal than the IOC GEOs. With a better ranging signal, CRW and CRE can be used as a ranging source to augment the number of GPS satellites available to users. This is especially important to mitigate service gaps caused by GPS outages or weakness of the GPS constellation.

Another reason for replacing the IOC GEOs was to address the fact that they were approaching the end of their expected service life. The FAA typically leases GEO satellites for ten years. Depending on the circumstances, this lease may be extended, but toward the end of the lease, new GEO satellites are procured to replace the existing satellites. CRW and CRE replaced AOR and POR. CRW and CRE are now reaching end of life for WAAS and the FAA is pursuing the next set of GEO satellites. Eutelsat 177 West A (labeled as SM9) will replace AMR. The SES-15 satellite (S15) will replace CRW and a new seventh GEO (GEO 7) will replace CRE. SM9, S15 and GEO 7 will provide a wide bandwidth ranging capability. Refer to Figure 4 for the different GEO coverage footprints over the history of WAAS.

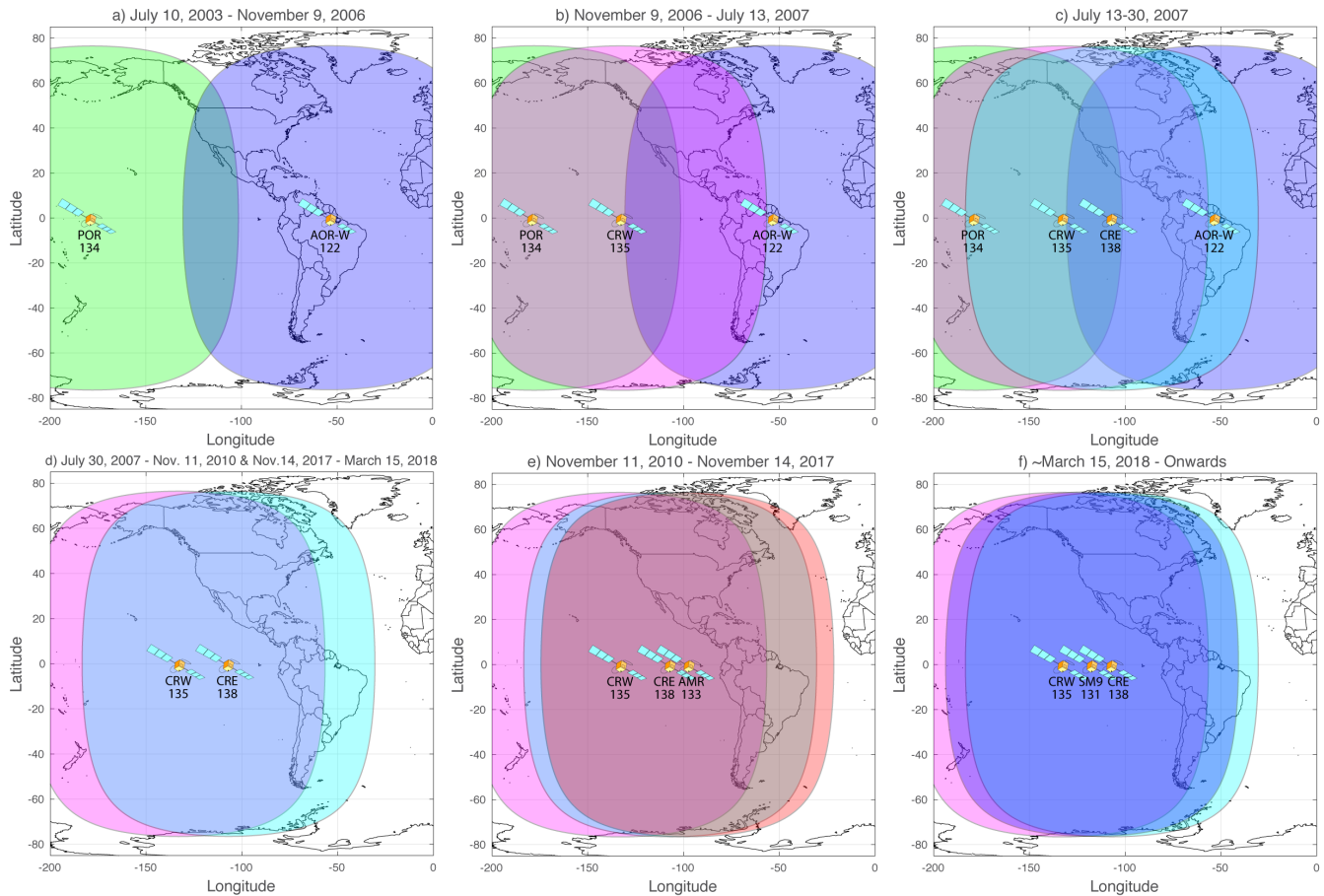


Figure 4. The different GEO coverage footprints over the history of WAAS.

Terrestrial Communication Expansion

The WAAS network communications infrastructure, known as the Terrestrial Communication Network (TCN), was designed to redundantly transport GPS measurement and navigation data from each of the geographically dispersed WRSs to each of the WMSs, to transport the to-be-broadcast WAAS user messages from the WMSs to the uplink stations, and to transport a variety of control and status information between all sites. The TCN uses a hub and spoke architecture consisting of four core communication nodes, two secondary communications nodes, and distribution routers at each of the WRS and GUS sites. This architecture is duplicated so that there are actually two fully redundant networks for transporting WAAS data. The core communications nodes were originally connected with 1.544 Mbps circuits and the connections from the core nodes to WRS and GUS sites were through 64 Kbps circuits. This bandwidth supported L1 and L2 measurement data only. In order to support the addition of L2C and L5 signal types and prepare for the eventual transition of the system into dual frequency capability, the network bandwidth was expanded. This expansion included upgrading to new router hardware as well as doubling communications line bandwidths to 128 Kbps for WRS sites and 3.088 Mbps for the core-to-core connections.

Tech Refresh/Maintenance

Every aspect of WAAS has largely been refreshed since IOC. The few exceptions are relegated to such items as equipment racks and antenna cables from the original IOC site installations. The refresh and maintenance of WAAS discussed in this section is structured by equipment, operating system/compiler, and maintenance/site relocations.

The concept for WAAS was to utilize to the fullest extent possible Commercially Available Off-The-Shelf (COTS) products with the belief this approach would allow inexpensive updates and greater efficiency [6]. Over the lifetime of WAAS the reality has been a mixture of COTS, Non-Development Items (NDI), and custom developments specifically for the WAAS application. The more significant equipment refresh efforts were the reference receiver, antenna, and processor, along

with the associated Operating System (OS) and compiler. Other equipment refresh efforts more closely followed the COTS/NDI paradigm and included cesium clocks, communication routers, timing receivers and power conditioners to name just a few.

Reference Receiver

WAAS is currently using the third generation reference receiver with all three generations being developed and manufactured by NovAtel Inc. The first generation reference receiver was internally funded and developed at NovAtel and was essentially three independent receivers contained within the same chassis. The key differentiators for this receiver at its time were L1 C/A multipath mitigation provided by the Multipath-Estimating-Delay-Lock-Loop (MEDLL) and P-Code delayed correlation technology for semi-codeless L2 tracking. The 2nd and 3rd generation receivers (G-II and G-III) were directly funded and overseen by FAA. The G-II receiver had the same core L1 C/A and semi-codeless L2 tracking as the G-I receiver but other key features were added such as L1 C/A correlator outputs for Signal Quality Monitoring (see SQM in later section), improved RF interference rejection, and an expandable architecture so the receiver could be upgraded for GPS L2 C/A and L5 signal processing [7]. Ultimately, MEDLL processing was not used from this receiver and all WAAS GPS L1 C/A signal processing since has been based on 0.1 chip correlator measurements. The G-II's started fielding in 2005 and were fully deployed in WAAS with incorporation of the final Mexico and Canadian stations in 2007.

The G-III reference receiver was developed to address pending G-II End-of-Life concerns and incorporate additional signal processing needed for dual frequency operations. An important point of emphasis with this development was ensuring measurement performance closely emulated the G-II to minimize algorithm retuning. The receiver development also required compliance with RTCA DO-178B Level D software certification guidelines and meeting stability requirements. The G-III has the channel capacity to track 18 GPS satellites and associated L1 C/A, L1C, L2C, L2P(Y) and L5 signals and eight GEO satellites with L1 C/A and L5 signals. This reference receiver provides improved RF interference mitigation with pulse blanking (G-II had pulse suppression), adaptive carrier tracking, and improved robustness with almanac validation and Timing Receiver Autonomous Integrity Monitoring (TRAIM) functionality. To address lessons learned from G-II test and integration, the FAA added a test environment at six test sites at WRSs that allowed G-III data to be provided in place of operational measurements to a shadow C&V in order to more completely evaluate its performance. The G-III started fielding in WAAS in 2015 and completed deployment in 2016.

Reference Antenna

The reference station antenna used for the first few years of WAAS service was fielded just prior to IOC in 2003. The relatively late finalization of this antenna was caused by discovery during algorithm validation that the original antenna had unacceptably large bias errors in pseudorange as a function of azimuth and elevation. The antenna deployed at IOC was a NovAtel GPS-600 element integrated into the original WAAS assembly [8]. While this antenna addressed the critical spatial bias concerns, one of its performance limitations was poor L2 gain which resulted in signal acquisition at higher elevations (~8 degrees elevation vs. 2 degrees from the original antenna) and ultimately degraded performance since both L1 and L2P(Y) GPS measurements are needed for WAAS processing. The original antenna vendor, Micropulse, continued research on an antenna element that would provide acceptable spatial bias errors for WAAS and improve L2 gain performance. They were ultimately successful and jointly developed the current WAAS antenna with FAA which included more stringent spatial bias error limits (<25 cm at 5 degrees elevation) and a filter/low noise amplifier with L5 signal reception. This antenna was fully deployed by 2007 and is still in service today.

Processor

At the start of IOC, WAAS used three different types of processors for its various subsystems. The corrections processors and operations & maintenance processors at the WMS sites were IBM Model 397s, the WRS and GUS processors were IBM Model 43ps, and the safety processors at the WMS sites used custom hardware integrating single board computers equipped with Motorola MPC7400 processors. By 2009, all processor hardware, except for the safety processors, had been upgraded to IBM Model p615s. These initial upgrades were required to address performance needs and to address end-of-life concerns. In 2014, another upgrade was performed to replace the p615s with IBM Model 720s. This upgrade was primarily for end-of-life reasons. So far, all processors in WAAS have been based on the Power PC architecture. The first major upgrade of the safety processors since IOC is scheduled to occur in 2019. This will upgrade will address obsolescence and will increase performance in preparation for dual frequency improvements.

OS/Compiler

Refresh of the operating system and compiler was a significant undertaking that took place with the latest upgrade of the IBM AIX processors at all sites in the system. The most challenging aspect of the upgrade was outlining an efficient approach for testing all subsystems that still meets the requirements of DO-178B. The FAA was able to maintain the existing DO-178B design assurance and verification evidence associated with the Level D software while avoiding the excessive cost of performing a 100% re-verification of the Level D requirements. In order to minimize changes introduced during the processor upgrade, the only software changes allowed as part of the processor upgrade will be those changes necessary to support the upgrade and FAA directed minor changes such as antenna position updates. The focus of the analysis and verification efforts was on the impacts of the specific changes being implemented (processor/OS/Compiler) and their effect on the WAAS functional behavior. The goal of the effort was to perform sufficient analysis and verification to demonstrate that the behavior of the system using the updated system components (i.e., new processor, OS, and compiler) was consistent with the existing approved baseline, the WAAS Safety Case is preserved and the residual life-cycle risk is reduced to an acceptable level.

Maintenance

The WAAS antenna position updates represent one of the more important periodic maintenance activities. Fundamental to the integrity and accuracy of WAAS is the surveyed positions of the reference station antennas. At IOC there was no process for periodic resurvey of the antennas or an established criterion for how large antenna position errors could be before becoming an integrity concern. The WAAS Integrity Performance Panel (WIPP) [9] assessed that position error for each WAAS reference station antenna should be maintained to within 10 cm when measured relative to the International Terrestrial reference Frame (ITRF) datum for any given epoch. Mexico City was allowed to be within 25 cm given the significant subsidence at this location [10]. The ITRF datum version (realization) is the one consistent with WGS-84 and also used for positions of the GPS Operational Control Segment monitoring stations. The basis for these error thresholds was they were smaller than the antenna bias error, which can be as high as 25 cm for low elevation angles as mentioned above. Worst-case antenna bias errors are considered throughout the WAAS integrity analysis to ensure that all allocations still being satisfied. The reference antenna coordinates are assessed periodically with offline monitoring to determine the timeframe coordinates should be updated in the operational system to stay within thresholds. Generally, the WAAS antenna coordinates are updated on an annual basis.

Other significant activities that could be considered under maintenance are associated with site and equipment relocations. On a few occasions buildings where WRS equipment was located was deemed no longer viable or needed to be repurposed. On these occasions, relocation has required new site and multipath surveys and in some instances RF surveys. The planning for taking one set of equipment down and bringing on new equipment sometimes has resulted in WRSs being out of operation for several months until site verification is completed and the new antenna coordinates can be input. The Billings, MT and Cold Bay, AK WRSs both required relocation in the past 15 years.

Performance Improvements

In addition to expansion of the WRS network and fielding of equipment with better performance, WAAS has updated the algorithms that generate the corrections and corresponding confidence bounds. These updates were generally made to improve the accuracy of the corrections, to tighten the confidence bounds, and/or to address integrity concerns that may be identified. This section will describe the algorithm changes that were made primarily to improve WAAS performance. At the end of the section we will show the improvement to the coverage region provided by WAAS. The subsequent section will address changes that were primarily aimed at mitigating integrity concerns.

Correction Processor (CP) Tuning and Enhancements

One of the first performance upgrades after WAAS was commissioned addressed known anomalies that affected system performance and the ability to analyze other anomalies or performance of the system. Incorporation of software changes to the C&V CP capabilities were focused on improving continuity, availability, and accuracy as well as addressing current anomalies that were attributable to the current CP algorithms.

A summary of the CP enhancements follows:

Cross-thread cycle slip detection - The cross-thread cycle slip algorithm improved the ability to detect cycle slips that were missed by a polynomial fit. Furthermore, it helped prevent false cycle slip detections due to phase scintillation by loosening the cycle slip threshold in the polynomial fit when no cycle slip has been detected. The net effect was a sizeable gain in system availability.

Cross-thread pseudorange edit - This algorithm screens out pseudoranges with excessive multipath by comparing the pseudoranges received by a WRE pair for each satellite. This screening, when performed before CNMP, allowed both CNMP and the data editor to generate more accurate phase offsets by excluding multipath measurements from the phase-offset estimates. It also allowed WRE bias to generate a more accurate smoothed pseudorange difference, which directly affected the WRE bias.

WRE Bias - The WRE bias changes improved the ability to maintain a more consistent bias than the prior algorithms. Furthermore, the mean phase difference calculated in WRE bias allowed for cross-thread cycle slip detection on GEO satellites.

Code Noise and Multipath (CNMP) - The CP CNMP algorithm, when combined with data editor changes, improved the ability to screen out measurements with excess multipath and better characterize the data weighting used by the Kalman filters downstream. When combined, the better screening and more accurate data weighting led to higher overall system availability, as well as a noticeable improvement in the convergence of the ionospheric and orbit determination (OD) Kalman filters.

Orbit Determination Tuning - This consisted of a combination of software enhancements and the tuning of Operational System Parameters (OSP) in order to improve orbit accuracy, UDREs, availability, and address current software deficiencies.

Maneuver Detection Tuning - This change included modification to the maneuver detection software and OSPs in order to eliminate false GPS satellite maneuver declarations, improve the capability to detect true maneuvers earlier, and eliminate unnecessary processing. The change also protects the OD filter from being degraded due to a failure to recognize the maneuvering satellites.

Old But Active Data (OBAD) Mitigation - Changes were made in the CP to prevent users from experiencing excessive error when using OBAD, as well as OBAD alarms in Integrity Data Monitoring (IDM). The basic concept of all the OBAD avoidance algorithms was to limit the change in correction by the maximum acceptable error for any time within the window that the "old" correction could potentially be active.

Process Input Data (PID) Architectural Impact - The addition of new PID functionality resulted in some modification to the PID software architecture and some reordering of functions. The cross-thread pseudorange edit was the first new process, followed by cross-thread cycle slip, perform polynomial fit, code noise and multi-path, WRE bias, and the perform data editing. Also, the receiver data monitoring capability was replaced by the combination of the new screening capabilities and WRE bias algorithms.

SP CNMP

The SP CNMP monitor has undergone numerous modifications since IOC. The purposes of the CNMP algorithms are to estimate and correct for observed code noise and multipath, and then to provide a confidence estimate for residual error in multipath-corrected L1 and L2 pseudorange measurements. To perform this function, CNMP must check for cycle slips, data gaps, and other anomalous signal tracking conditions. The algorithm has continuously been presented with changing input conditions due to the deployment of different reference station hardware at varied locations with significantly different environmental factors. The algorithm has undergone many improvements to improve its performance both under nominal and challenging conditions [4].

The most important robustness measure added to CNMP was processing all three threads in the SP and then taking advantage of data editing across threads. Cross thread pseudorange editing in particular allowed mitigation of large multipath errors that sometimes resulted in CNMP not passing its bounding requirement at the most challenging multipath sites. This added logic checked pseudorange between threads taking into account geometry differences between antennas

and satellites as well as average clock differences between threads and compared to a threshold. If the difference exceeded threshold it was excluded from CNMP processing. The algorithm also included isolation logic in an attempt to determine which thread had the offensive measurement. This logic was also extended to comparing carrier phase to further isolate cycle slips. This was especially important with northern latitude stations added from Alaska and Canada where phase scintillation can present very challenging tracking conditions for L2P(Y) processing [11]. The full cross thread edit logic was added in the 2007 timeframe [4]. In addition to this editing, several specialized detection algorithms were added overtime to assist with anomalous carrier tracking that was found to be common mode. These conditions were sourced to strong phase scintillation and in one instance, special GPS operations with increased P-Code signal power.

The modifications to CNMP mentioned above were intended to improve conditioning of measurements so that downstream integrity monitors would have more accurate and consistent range measurements on which to operate. One of the recent modifications to CNMP was to remove the conservatism in GPS processing that assumes at the start of track worst case multipath is always present. This assumption inflates the initial error uncertainty sigma value. Generally this inflation is not needed. The new logic utilizes information from cross thread processing to make a determination on the multipath environment for each satellite track. The algorithm keeps track of instances when both L1 and L2 pass cross thread pseudorange edit to determine if the multipath history is benign. If this history is benign and the satellite elevation angle is above 30 degrees then CNMP error bound is allowed to start at a lower sigma value. This change has demonstrated benefit for satellite anomalies such as PRN 21 where it suffers periodic jumps in phase that cause CNMP to restart at all WAAS reference stations [12] or in phase scintillation environments at stations on the fringe of WAAS coverage. The other significant performance enhancement with CNMP has been for GEO satellite processing. This change recognized that wider bandwidth GEOs and 0.1 chip receiver tracking results in smaller worst case multipath than had been assumed with IOC. The initial unsmoothed CNMP upper bound sigma value for the GEOs was reduced from 30 to 10 meters. These tighter confidence bounds result in the broadcast UDRE for the GEO satellites reaching the floor value of 7.5 meters in approximately 5 to 6 hours instead of taking more than one day.

UDRE Monitor

The portion of the UDRE monitor that evaluates the GPS satellite corrections has not changed significantly since the original IOC build. In order to compute a useable UDRE for a satellite, a minimum of three WRSs have to return valid measurements to that satellite. In the IOC build, at least one observing WRS had to be within CONUS in order to send a UDRE value below 50 m. This restriction originally had little impact as 20 of the 25 WRSs were within CONUS. However, the anticipated addition of 13 more WRSs outside of CONUS would cause this rule to severely limit the anticipated performance improvement. It was recognized that the restriction was not actually necessary in order to maintain integrity and was removed from the UDRE algorithm in 2005, before the fielding of the new stations. Thresholds on the allowed variation arising from tropospheric uncertainty was increased due to some false alerting caused by the new Alaskan WRSs, and the calculation of the integrity risk was made slightly more conservative (occasionally resulting in larger required UDRE values), but otherwise the GPS satellite algorithms are largely unchanged.

In contrast, the algorithms that evaluate GEO satellite corrections have undergone more significant changes. Originally, WAAS only sought to have the UDRE bound the GEO ranging error within the U.S. airspace. However, it was recognized that users outside of this airspace do not have a means to identify whether or not the bound applies to them. As a result the minimum allowable broadcast UDRE values, the UDRE floors, were increased from 7.5 m to 15 m for AOR-W and from 15 m to 50 m for POR in 2006. The MT28 parameters [13] for the GEOs were originally set so that the projected error bound was the same everywhere throughout the footprint. These values were changed to a fixed set of parameters that reflected increasing uncertainty for users farther away from the center of the WRS network. These new fixed GEO MT28 parameters were fielded in 2007 along with changes to the UDRE calculation to have it overbound all errors within the GEO footprint. Finally, the algorithm that evaluates the safety of the fixed GEO MT28 parameters in real-time was improved in 2008, removing some unnecessary conservatism. These updates, combined with the change from narrow bandwidth to wide bandwidth GEOs, allowed the reduction of the GEO UDRE floors back down to 7.5 m

There are more recent efforts underway to significantly update the UDRE monitor. This new version, labeled covariance UDRE, envisions a more integrated determination of the UDRE and MT28 parameters [14][15]. The current algorithms determine the UDRE value and the MT28 parameters separately. This separation is not optimal as certain conservative measures may be required in each part to account for possible behavior in the other part. The covariance UDRE algorithm

should be able to provide tighter error bounding on both the GPS and GEO satellites and allow WAAS to dynamically update the GEO MT28 parameters.

GIVE Monitor

In contrast to the UDRE monitor, the GIVE monitor has undergone significant changes and improvements since IOC. The IOC version used a simple planar model for the local ionosphere around each IGP. It also created the concept of a storm detector to distinguish between quiet ionosphere that could be well-modeled and disturbed ionosphere that required a much larger error bound [5]. When the ionosphere was quiet, the IOC GIVE algorithm applied a significant inflation factor, called R_{irreg} , to allow for the possibility that the ionosphere was nearly in the disturbed state. It also included a threat model to account for ionospheric anomalies that might not be adequately sampled by the distribution of WRS measurements [16]. This so-called undersampled threat model was empirically derived using the worst collected ionospheric data prior to 2003. Part of this threat model also described the largest historical ionospheric delay as a function of time of day and geomagnetic latitude. It exploited the fact that the ionosphere should never have a large delay, at certain times and in certain regions, in order to lower the corresponding GIVEs.

Shortly after IOC commissioning, two of the most significant ionospheric disturbances ever to be sampled with dense GPS data occurred; one in October 2003 and the other in November 2003 [17]. WAAS maintained its integrity throughout these events, but many of the underlying models in the GIVE algorithms and threat models required revisiting. Large ionospheric delays were observed at very high geomagnetic latitude. It was decided to remove the algorithm that could put a ceiling on the GIVE based on the expected maximum Vertical Total Electron Content (VTEC). This max VTEC algorithm was removed in 2006. The undersampled threat model also required revision, however, it was found that using the IOC methodology would lead to a significant reduction in WAAS coverage. It was therefore decided to expand the idea of the storm detector to further identify the more significant storms such as the two that occurred in 2003. These events, now labeled extreme storms, are very rare but when they do occur, isolated pockets of disturbed ionosphere can persist for hours afterwards. These isolated pockets can temporarily escape sampling by the WRS measurements, leading the GIVE algorithm to mistakenly declare the ionosphere to be in a smooth and quiet state. An Extreme Storm Detector (ESD) was created to specifically react to these rare events. An extreme storm is declared only if very large disturbances are observed for an extended time. However, once an extreme storm is declared, all GIVE values are set to maximum until at least eight hours after no further disturbances are detected. Thus, an ESD trip will prevent WAAS from providing precise vertical guidance for at least half a day. The benefit is that the undersampled threat model when the ESD has not tripped can be dramatically reduced. The implementation of the ESD and the inclusion of the 2003 and 2004 storm data into the threat model took place in September 2007.

Also included in the same update was a reduction to the R_{irreg} inflation term. Rather than assuming that the ionosphere was always in a near storm state, an updated algorithm, termed dynamic R_{irreg} , utilizes the actual measured level of disturbance [18]. As the ionosphere is in a very quiet state the vast majority of the time, this inflation factor is significantly reduced. Unfortunately, this reduction exposed a weakness in the IOC algorithm. For simplicity, R_{irreg} multiplied both the ionospheric modeling uncertainty and the measurement noise uncertainty. This simplification was usually very conservative for static R_{irreg} , but was less so under dynamic R_{irreg} . A new more complicated analysis was created that correctly treated these two error sources separately, creating a new measurement noise inflation term, R_{noise} [19]. Fortunately, this new analysis was able to retain the majority of the GIVE reduction provided by dynamic R_{irreg} while maintaining the required level of integrity. The change to R_{irreg} and inclusion of R_{noise} meant that many of the thresholds and parameters in the GIVE algorithm were not tuned to their optimal values. A subsequent round of tuning identified better parameter values that led to a significant GIVE reduction when they were fielded in September 2008.

Another significant improvement to the GIVE monitor came from the introduction of kriging [20] [21] [22]. Kriging is a technique adapted from geospatial statistics to more accurately model the vertical ionospheric delay at the IGPs. The kriging GIVE algorithm models the ionosphere as having an underlying planar trend with an added stochastic variation similar to the IOC algorithm. The main difference is that kriging assumes that the stochastic error is correlated spatially (the IOC algorithm treated it as though the stochastic component was completely independent of location). Kriging accounts correlated ionospheric delay variations between each measurement and the IGP as well as from one measurement to another. The model of the spatial uncertainty, called the variogram, has a non-zero value at zero separation distance and then increases as the distance between two points increases. Kriging better models the local variations in the vertical

ionosphere than did the IOC algorithm. This allows the GIVE monitor to function under increasingly disturbed states, creating more accurate estimates without triggering any of the storm detectors. Thus, minor and medium disturbances in the ionosphere that would lead to storm detector trips and outages in the vertical guidance service, were much less likely to trip with kriging, leading to significant availability and continuity gains for this service.

MSD

With the majority of the threats from the October 2003 storm removed by the addition of the ESD, a second extreme storm became the driver of the WAAS threat model. On November 20th and 21st, 2003, a plasma jet emitted from the equatorial region creating an extremely sharp gradient which extended throughout the eastern half of the US, culminating in the great lakes region. Unlike other extreme storms, the gradient of this storm was shown to be sharp enough that an event such as this could go undetected when different subsets of the WAAS measurements were excluded. Thus, the threats from November 21st were included in the ESD threat model.

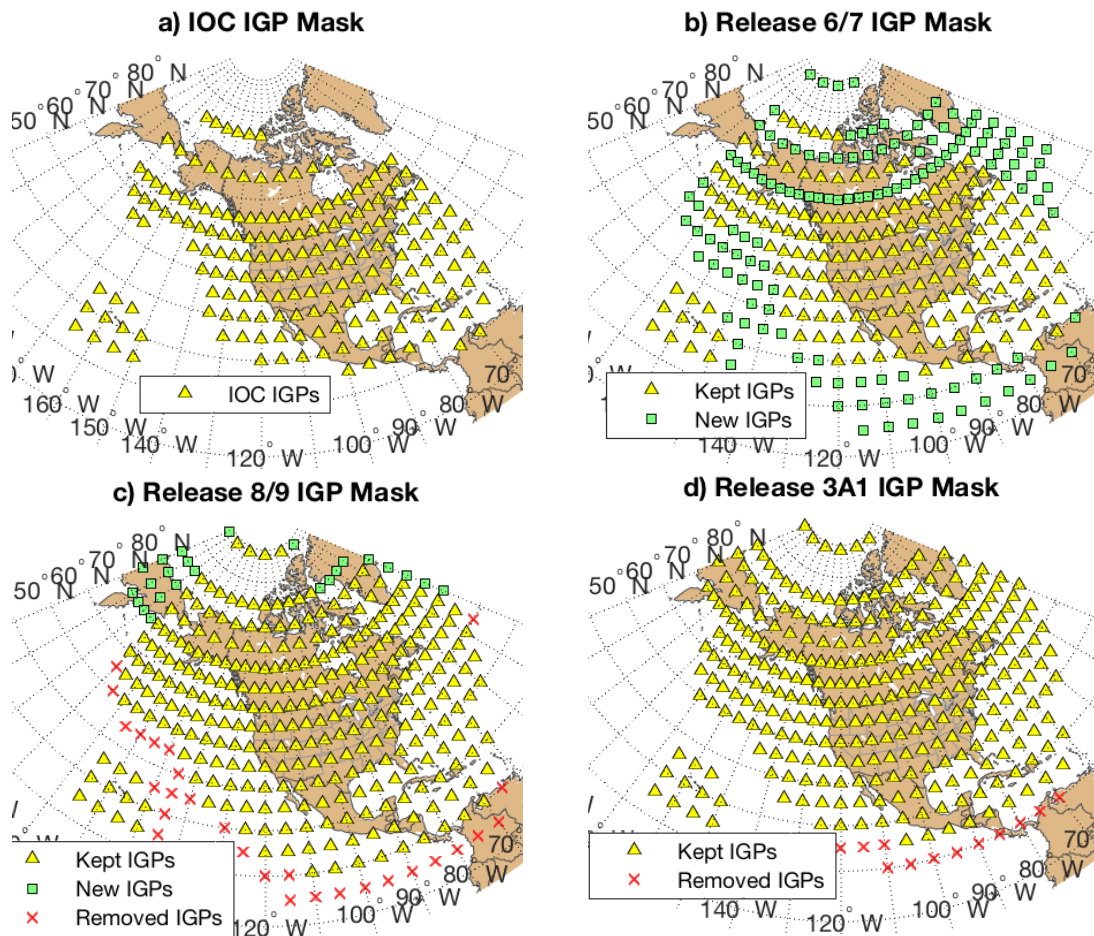


Figure 5. The different IGP Masks over the history of WAAS.

Analysis of a periodic GIVE spike was shown to be driven by the threat model and in particular, the critical points in the threat model attached to this November 21st, 2003 storm. Deeper analysis of the storm on November 21st, 2003 showed that the maximum chi-squared value of the system, which is the metric that trips the ESD, increased gradually and significantly for the November 21st storm. This behavior drove the design for a Moderate Storm Detector, which was modeled after the ESD algorithm but with a smaller threshold and a short outage time [23]. As with the ESD, the MSD allowed threats to be removed at an even higher rate, improving the performance even more than with the ESD. The MSD thus detects less extreme storms, and in the event that no storm is present, the threat model remains extremely small. Thus the ionospheric conditions were split into three states: quiet, moderately disturbed, and extremely disturbed. By separating out the truly quiet from the moderately disturbed an even smaller threat model could be applied most of the

time. When the MSD trips, but the ESD does not, the previous threat model is used, leading to still very good service, but with some reduction in coverage and when the ESD trips, vertical guidance is no longer provided, but horizontal guidance is provided under all ionospheric conditions.

IGP Mask

The IGP mask for WAAS has also changed over time. Figure 5 shows the mask at four different stages of operation. Figure 5a shows the original IOC mask with 190 IGPs, primarily serving the CONUS region. The IGPs around Hawaii transmit the estimated ionospheric delays, but their GIVEs are always set to not monitored. The NM setting is due to having only one WRS in Hawaii and no other receiver measurements overlap this region. The lack of redundancy means that the system cannot fully rule out receiver faults from affecting the grid estimates. Nevertheless, the estimates are generally accurate and may be used for non safety-of-life applications. Figure 5b shows the dramatic expansion to the mask that occurred in 2006 when 131 IGPs were added to the mask. This larger number includes denser grid spacing above 55° N, which allows better accuracy and lower GIVEs above Canada and Alaska. In 2008 some of the westernmost IGPs were removed from the mask, as they were almost never monitored. Further, the southernmost IGPs were also removed due to equatorial ionospheric behavior observed in that region. Additional IGPs were added in the north to provide better availability for Alaska and Canada. Figure 5c shows these changes resulting in a mask containing 317 IGPs. In 2010, an additional 12 IGPs were removed from the south again due to issues with modeling the equatorial ionosphere. The current mask with these changes is shown in Figure 5d.

In 2008 some of the westernmost IGPs were removed from the mask, as they were almost never monitored. Further, the southernmost IGPs were also removed due to equatorial ionospheric behavior observed in that region. Additional IGPs were added in the north to provide better availability for Alaska and Canada. Figure 5c shows these changes resulting in a mask containing 317 IGPs. In 2010, an additional 12 IGPs were removed from the south again due to issues with modeling the equatorial ionosphere. The current mask with these changes is shown in Figure 5d.

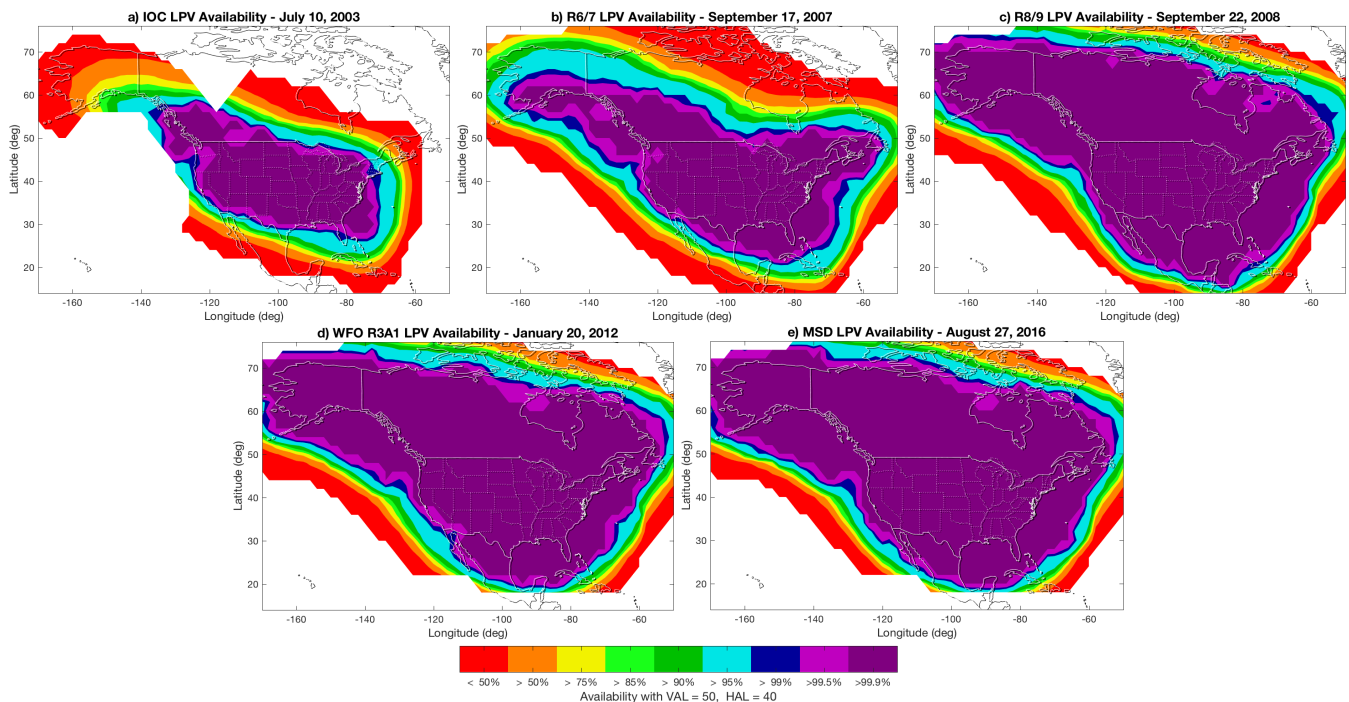


Figure 6. Coverage areas of LPV at different times since WAAS commissioning

Availability Improvement

To examine the performance improvement provided by these enhancements, we have used our Matlab Algorithm Availability Simulation Toolset (MAAST) [3]. This toolset uses the WAAS reference station and satellite locations to determine which measurements should be available to WAAS at any given time and then emulates the WAAS algorithms to estimate the expected UDRE and GIVE values. These values are then used on a simulated grid of users to estimate the expected protection level values and resulting availability. It has been found that MAAST is able to very accurately estimate the UDRE and GIVE values and is an invaluable tool to identify the impact on performance due to proposed algorithm or reference station. Figure 6 shows the WAAS Localizer Precision with Vertical guidance (LPV) coverage areas over its history. LPV is an approach procedure similar to Category I precision approach that is able to guide an aircraft to within 250 feet of

the ground [24]. It requires that the Vertical Protection Level (VPL) be below 50 m and the Horizontal Protection Level (HPL) be below 40 m. The dark purple regions of Figure 6 show areas where 100% availability of LPV is predicted by MAAST, which has found to also accurately match the actual performance obtained after each WAAS update. As can be seen in the figure, the coverage area has expanded significantly over the years.

In order to distinguish WAAS improvements from changes to the GPS constellation strength, all of the plots in Figure 6 were calculated using the standard 24 satellite GPS constellation specified in Appendix B of [25]. Normally, MAAST is run using almanacs corresponding to the GPS constellation for the day being simulated. However, while the constellation strength has generally improved from 2003 to the current day, there can be outages and other variations that lead to noticeable changes in coverage. By using the same reference constellation for all plots, we can separate the amount of change due to WAAS modifications from those due to constellation changes. This standard 24-satellite constellation often has somewhat worse performance than the actual constellation since it usually has 31 operational satellites. However, it is not uncommon for there to be times where the reference constellation does outperform the actual one.

As identified in previous sections, WAAS has fielded many improvements over time and in this section the focus is on availability after fielding of the most significant algorithm updates. WAAS development was broken into several phases with Phase II commencing after IOC. Figure 6a shows the coverage that was initially available after IOC. Much of CONUS had good availability, but there were limitations towards the edges and there was very limited availability in Alaska. Phase II followed IOC and originally envisioned 10 software releases. Over time various planned builds were sometimes merged together and/or split into multiple releases that sometimes resulted in creative release names (see the appendix for a full list of these upgrade activities). Some software releases addressed primarily maintenance activities with little impact on performance and others included major algorithm updates. The first major algorithm update was included in Release 6/7 that was fielded on September 17, 2007. This release included dynamic R_{irreg} , ESD, and a much denser ionospheric grid north of 55° N latitude. In addition to the algorithm changes, this release introduced two Canadian and three Mexican WRSs. Prior releases had replaced AOR and POR with CRE and CRW, and included the four additional Alaskan reference stations. Figure 6b shows the improvement in the coverage area after this set of changes. There is significant improvement in the coverage region, particularly on the East Coast.

The next major algorithm upgrade occurred on September 22, 2008 when Release 8/9.2 was fielded. This release included a retuning of the GIVE algorithm parameters to exploit the R6/7 algorithm changes, and a removal of some unused grid points. The prior release introduced the final two Canadian and two Mexican WRSs. The retuning in particular resulted in a significant expansion of the coverage to now provide high availability through most of Alaska, Canada and northern Mexico as shown in Figure 6c.

The next phase of WAAS development, Phase III, started in 2009 [2]. Under this WAAS Follow On (WFO) effort the release names were restarted at 1 and underwent similar reorganization and name changing over time. The next major algorithm change was introduced on October 20, 2011 with WFO Release 3A. This release included kriging and corresponding threat model changes. Also the AMR satellite was introduced shortly before this release. Subsequently, Release 3A1 was fielded on January 20, 2012, to remove some of the southernmost grid points over Mexico due to poor modeling of the equatorial ionosphere. These changes are shown in Figure 6d and led to better coverage in Alaska, but somewhat worse performance on the West Coast and southern Mexico. The kriging however did prevent several ionospheric disturbances over the subsequent years from tripping the storm detectors. This source of availability improvement is not represented in the MAAST modeling.

A new phase of WAAS development began in 2014 [2] and with it came a new naming convention for releases that were now linked to Calendar Year (CY). The most recent algorithm change introduced the MSD with Release CY16. This change was introduced specifically to improve coverage on the West Coast. As can be seen in Figure 6e, the algorithm was successful in meeting its goal although in practice, we sometimes lose this coverage due to the actual constellation strength (or lack thereof).

Integrity Improvements

In addition to the performance improvements identified in the previous section, sometimes new integrity concerns were identified that required algorithm changes that led to a degradation of service. These changes were required due to an improved understanding of the risks. However there was a desire to avoid degrading service. Fortunately, the above improvements were able to offset and overcome any reduction in coverage that would have resulted from fielding the following design changes in isolation.

WAAS Integrity Resolution Process (WIRP)

As WAAS was being developed, it became clear that a process for tracking, assessing and evaluating integrity issues was needed. At the time of commissioning, all known threats were sufficiently mitigated. However, as WAAS offline monitoring commenced [10] and as new and better understanding of the integrity risks became clearer, concerns arose that needed to be managed in some way. The WIRP was developed to provide an efficient means to address integrity threats against the fielded WAAS and a process for them to be properly evaluated. Integrity threats are assigned to nodes on the fault tree and previously an integrity threat either met its Probability of Hazardous Misleading Information (PHMI) allocation or failed. If and when an integrity issue surfaces, a problem report is issued. The matter is deliberated, and if deemed sufficiently hazardous, a Hazard Record is issued with an associated determination of risk and acceptable exposure time. These values will determine the course of action and the time frame in which the issue needs to be addressed. Higher risk items with short exposure windows need to be addressed quickly, potentially through operator action or an expedited change to an algorithm. Lower risk items with longer exposure windows can be addressed by deeper algorithm changes

SQM

Signal deformations are caused by imperfections in the broadcast code chips transmitted by the satellites. Rather than being perfectly square waves with upward and downward transitions occurring exactly when desired, the chips have variations in the rise and set times, finite transition slopes, containing overshoot and oscillations. These imperfections can be further exacerbated by behavior of the receiver front-end filters and tracking loop design [26] [27] [28]. This error source was first noticed on SVN-19 where two different receivers observed meter level differences due to deformations in the broadcast code chips [29]. The threat model for this type of threat was very much under investigation during the initial design and fielding of the WAAS reference receivers. It was believed that comparing measurements from the two tracking loop implementations that first observed the SV-19 threat (i.e. narrow versus wide correlator spacing) would be sufficient to mitigate the threat. However, as the threat space became better defined, it became clear that more correlator measurements would be needed along with a more sophisticated detection algorithm. Unfortunately, it would take a few years to design and field this new receiver along with the new Signal Quality Monitoring (SQM) algorithm. Work was conducted with the receiver manufacturers prior to 2003, to better understand their receiver designs and how they would compare against our reference receivers. The understanding gained from this effort was that early user receivers were sufficiently similar to temporarily use a reduced version of the threat model. It was determined that the remaining risk was adequately covered by the broadcast UDRE values and that it would be acceptable to take no more than five years to field an algorithm capable of protecting any MOPS compliant receiver design against the full ICAO threat model. The CCC monitor provides protection against any sudden changes in the broadcast chip shape from any satellite.

The second generation of receivers provided measurements at nine different correlator spacings. An algorithm was designed that evaluated the symmetry and consistency of the chip shapes broadcast by the different satellites [26]. Initially this algorithm was used to evaluate performance off-line in order to ensure there were no latent harmful deformations. Over time, the algorithm was evolved to become more sensitive and less likely to lead to false alerts. The first version of this algorithm was fielded in September 2008. It uses four metric values to evaluate the differences among the satellite. A common mode shape distortion would lead to identical pseudorange errors on all satellites. Such an error mode would only affect the user clock estimate and not lead to a position error. Therefore, the monitor determines and removes a common mode shape and the metrics are only affected by differences from one satellite to another. When any one of metrics exceeds its threshold, the satellite is flagged as unusable. This flag persists for twelve hours after the metric returns below the threshold. The magnitude of the threshold is a function of the UDRE determined by the UDRE monitor.

The satellite signals are not all identical. There are nominal differences that create a persistent low level of distortion on each satellite. These nominal deformations lead to small biases on each satellite. A significant effort has been made to determine the upper bounds on the deformation errors as a function of the metric values. An offline analysis has

determined the maximum acceptable bias and therefore the appropriate threshold value for each UDRE. Since the initial version of SQM, it has undergone tuning to reduce the incidences of false alerts. No harmful signal deformation faults have occurred since WAAS commissioning, although some smaller changes have been observed [27] [28]. Improved outlier rejection was added to reduce the risk of multipath from excessively inflating the metrics. Some of the higher signal power tests run by GPS has created apparent differences and false alerts. Improved modeling of the potential SQM errors allowed the thresholds to be increased.

Ionospheric Threat Model Updates

The initial WAAS ionospheric algorithms were outlined in the seminal 2000 paper “Robust Detection of Ionospheric Irregularities” [5]. Among these algorithms was the ionospheric delay estimation at an IGP, which computed a weighted average of ionospheric Pierce Points (IPPs) in the vicinity of the IGP. The formal error of this fit was used as a major component of the GIVE, however it was clear that there were some errors larger than 5.33σ which was problematic in that the GIVE was expected to bound to 10^{-7} . As such, a second term, was added to the GIVE equation which ensured that the GIVE bounded all ionospheric irregularities [16]. As this term was generated by removing large fractions of the data set and testing the ionospheric algorithms against removed data, it became known as the undersampled term. This term is a simple lookup table using IPP density (measured in terms of the maximum radius of the furthest IPP from the IGP) and a Relative Centroid Metric (RCM). The threat model is then computed by employing a data deprivation scheme in that some subset of the data is removed before the algorithms are applied, and all of the data is then tested.

Initially, the data deprivation schemes were an annular scheme, four half planes and four three quadrant schemes. After the October 31st and November 21st 2003 storms, the data deprivation schemes were updated to reflect more realistic threats. A single station plus two point removal is used to create large gaps in the IPP distribution to test for localized disturbances, and directional deprivation, where several stations are removed successively from one (of eight) directions. All IGPs are tested for the duration of the ionospheric disturbance.

The WAAS ionospheric threat model is one of the most significant drivers of performance, and as such, much work and many updates have been done. The updates include those that improve performance, such as IGP mask updates and new ionospheric algorithms, and those that degrade performance such as adding new ionospheric storms to the overall threat model. On September 17th, 2007, the new storms from 2003 were added along with other ionospheric algorithms. This represents the first and only time new storms have been added to the threat model, however a large update is planned for CY18 which will include UIVE culling, a scheme for removing threats which cannot manifest themselves for any user. As part of the CY18 update, the solar cycle 24 storms will be included.

RDM

The RDM evaluates the performance of the satellite and ionospheric corrections together on each WRE line of sight. It does not use the internal IFB and TGD estimates from the CP and therefore is able to detect errors in these values that may not be detected at the UDRE or GIVE monitor. It also does not use the CP estimated WRE clock biases. Instead it determines its own estimates of the WRE clock biases using the corrected pseudorange residuals based on the surveyed location of the WRE antennas. In the IOC version this clock estimate used all corrected measurements in view of each WRE. Further, the RDM used significantly reduced versions of the proposed UDRE and GIVE values for weighting and internal threshold determination. When the new WRSs were fielded in Mexico, it was found that some southward looking measurements started to sample the equatorial anomaly region of the ionosphere. The broadcast GIVE values excluded these measurements, as they did not follow the internal models. However, the RDM did use these measurements with less conservative internal GIVE values. Unfortunately, these measurements occasionally corrupted the RDM WRE clock estimates, which in turn led to the flagging of multiple satellites as unusable. Two updates were put in place to address this issue. First, the RDM clock estimate incorporated measurement screening to remove outlier measurements. Second, the internal RDM GIVE values were increased for measurements that were at risk of passing through the equatorial anomaly. These fixes prevented subsequent false alerts by the RDM.

UPM

The UPM examines the corrections and looks to see if correlated errors exist to create a larger position error than expected. Like the RDM it uses internal less-conservative versions of the UDRE and GIVE for evaluation. The principle being that checking against small thresholds would provide an early alert compared to users who apply the much larger broadcast

UDREs and GIVEs. However, before IOC it was discovered that corner cases existed where the UPM did not always guarantee protection. Thus, it was left in as a final check, but it was not strictly required to meet integrity. Instead, a separate off-line analysis was performed to determine that adequate margin existed in the UDREs and GIVEs, to protect against simultaneous correlated errors. Recently, a new UPM algorithm was developed that does guarantee the user protection against the correlated error threat [30]. This new algorithm uses the broadcast UDREs and GIVEs rather than having to create reduced internal versions. It performs a chi-square check on the sum of the square of the normalized corrected residuals at each WRE. A mathematical proof shows that users will be protected as long as this chi-square metric is below a specified residual. This new chi-square UPM was fielded in 2017. At the moment, no integrity credit is taken for this monitor. However, in the future, the UDRE and/or GIVE values may be lowered, to exploit the protection now provided by this monitor.

WAAS Approaches and Equipage

When the FAA commissioned WAAS in 2003, a paradigm shift occurred for the precision approach services offered by the FAA. Instead of having local systems service an airport or single runway, there was now one system that provided service to the entire National Airspace System (NAS). Aviators could use WAAS to fly vertically guided approaches to many airports the first day WAAS was available. On that first day there were over 300 LNAV/VNAV Instrument Approach Procedures (IAP) published. As of late 2017, the number of IAPs that use WAAS has grown to over 4000 in the NAS.

The first LPV IAPs were also published in 2003. Though the number was small (only five), that number has grown significantly over the 15 years of WAAS operation. Each year since 2003, the FAA’s goal was to publish at least 400 new WAAS IAPs per year, and this number was always met and many times exceeded. Figure 7 shows the growth in the number of IAPs over the years. At first, IAPs were published primarily to airports and runway ends that have an existing ILS. However, there are now almost 2,700 LPV IAPs published to non-ILS runways compared to about 1,100 LPV IAPs published to runways with an existing ILS.

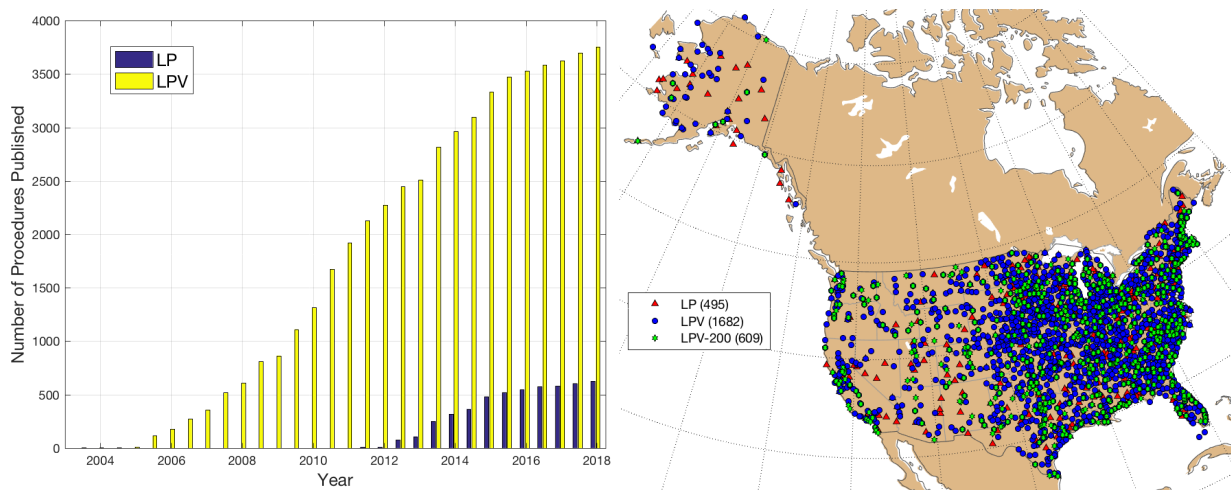


Figure 7. Number of published LP and LPV/LPV-200 procedures published since 2003 and their locations

Another improvement to the type of IAPs published was the establishment of the so-called LPV-200 IAP [31]. By definition, LPV IAPs would not go a decision height any lower than 250 feet. However, after extensive analysis and international coordination with ICAO, WAAS (and other SBAS’s) were approved for IAPs that went to a 200-foot decision height. The analysis included work by the FAA that included simulations, data analysis for a 3-year period, and other evaluations. The result of this work was that the FAA began to publish LPV-200 IAPs in early 2007. Ten years later, there are over 1,000 LPV IAPs published to a decision height of less than 250 feet (i.e. those classified as LPV-200 IAPs).

In 2009, another type of approach procedure was created: the Localizer Precision (LP) approach. This procedure was created for runway ends where terrain and/or obstacles do not allow the publication the glideslope portion of the approach. An LP procedure is one where the pilot may fly along a constant altitude rather than at a constant descent angle.

The tight lateral protection offered by WAAS allows LP IAPs to achieve lower decision altitudes than traditional non-precision approach procedures.

Figure 7 also shows a map of the airport locations that have LP, LPV, and LPV-200 IAPs. The additional improvements to WAAS availability and coverage have allowed more IAPs have been published. The FAA first published LPV-200 procedures in CONUS, but there are now LPV-200 procedures in Alaska. LPV approaches are located on the GPS (RNAV) approach charts. There is a line of minima for LPV. To know whether an LPV approach is LPV-200, the decision height must be below 250 feet. That is, there is no LPV-200 distinction on an approach plate, only the LPV line of minima is shown. Figure 8 shows the LPV-200 coverage region over time. As was the case for LPV performance shown in Figure 6, the LPV-200 coverage area increased significantly over time. Note that LPV-200 approaches were not published prior to 2007. As of January 4th, 2018 there are 655 LP procedures at 495 airports and 3,872 LPV procedures at 1,888 airports including 1029 LPV-200 approaches at 609 airports.

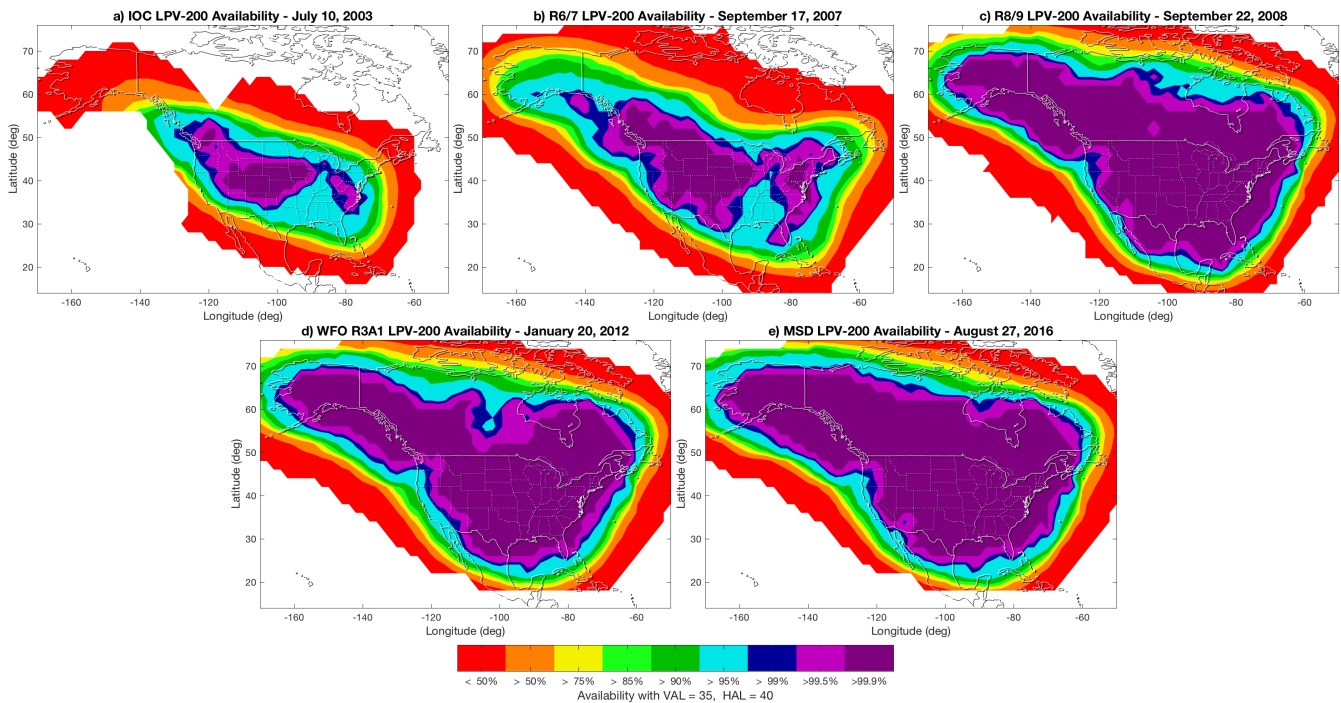


Figure 8. Coverage areas of LPV-200 at different times since WAAS commissioning

Figure 8 shows the LPV-200 coverage region over time. As was the case for LPV performance shown in Figure 6, the LPV-200 coverage area increased significantly over time.

The previous WAAS MOPS, D0-229D, was first published in December 2006. This version of the MOPS was later updated (to DO-229D Change 1) in 2013 and a subsequent update, DO-229E was published in late 2016. Because a sharp increase in the number of WAAS MOPS compliant aviation receivers were sold in 2007, it can be inferred that most of the avionics in use today are DO-229D compliant. Largely based on the WAAS MOPS, the FAA published a Technical Standard Order (TSO) that describes the FAA requirements for WAAS avionics. TSO-C145 (“Airborne Navigation Sensors using GPS Augmented by WAAS”) and TSO-C146 (“Airborne Navigation Sensors using GPS Augmented by WAAS”) are the two documents the FAA has published based on the WAAS MOPS.

The FAA estimates that over 100,000 aircraft are equipped with the WAAS LPV capability. The usage of WAAS provides a large safety benefit – vertical guidance is available to pilots that didn’t have that capability before. In addition to the large usage of WAAS by the general and business aviation community, SBAS is also gaining acceptance with air carriers. The first scheduled service air carrier to utilize an LPV approach occurred in 2009.

The FAA has encouraged avionics manufacturers to include the WAAS capability in their aircraft. For example, the FAA has contracted with CMC Electronics to provide WAAS capable avionics, with the LPV functionality, in the FAA's Research and Development aircraft. Including WAAS in the FAA aircraft assists in support of flight testing other programs, such as ADS-B.

Summary and Conclusions

WAAS has undergone many changes in its fifteen years since commissioning in 2003. These changes were in response to a variety of needs. The system needed to be maintained so as equipment aged and risked becoming less reliable replacements were undertaken. Some changes were in response to improving the operation of WAAS. Some were in response to integrity concerns that were identified after the initial commissioning of WAAS. The most obvious changes were the performance improvements that were put in place to expand the LPV and LPV-200 coverage regions.

WAAS is never static. The hardware and software are constantly evolving. Even as new geostationary satellites are brought online, plans for their eventual replacement are already being formulated. New levels of service have been created and new flight procedures are developed and published. This paper serves as a record of the most significant of these changes. After its commissioning in 2003, WAAS performance was primarily limited to CONUS. In the years that followed that service was expanded to Alaska, Canada, and Northern Mexico. The service also became more reliable and capable of providing vertical guidance to within 200 feet above the ground. WAAS continues to evolve as newer generations of equipment are fielded and new algorithms are developed. The purpose of these updates is to continue to provide vertical and horizontal guidance over a greater coverage region and with increasing reliability.

Acknowledgements

The WAAS program has benefited from significant contributions across Government, Industry and Academia and acknowledging individual achievements could be a paper in its own right. Instead, we have chosen to recognize the FAA Program Managers from IOC to present since their leadership and devotion was absolutely required for WAAS to be fielded and evolve to what it is today. To this end, Mr. Leo Eldredge at IOC, Ms. Deborah Lawrence through 2009, Mr. Deane Bunce through 2016, and currently, Mr. Don Wilkerson. We would also like to acknowledge Mr. Tom McHugh who was the WAAS Technical Director for almost this entire period.

References

- [1] Enge, P., Walter, T., Pullen, S., Kee, C., Chao, Y.C., and Tsai, Y.J., "Wide area augmentation of the Global Positioning System," Published in Proceedings of the IEEE, Vol. 84, No 8, pp.1063 - 1088, DOI: 10.1109/5.533954.
- [2] Lawrence, D., Bunce, D., Mathur, N. G., and Sigler, C. E., "Wide Area Augmentation System (WAAS) - Program Status," Proceedings of the 20th International Technical Meeting of the Satellite Division of The Institute of Navigation (ION GNSS 2007), Fort Worth, TX, September 2007, pp. 892-899.
- [3] Jan, S., Chan, W., and Walter, T., "MATLAB Algorithm Availability Simulation Tool," Published in GPS Solutions, Vol. 13., No. 4, September 2009.
- [4] Shallberg, K. and Sheng, F., "WAAS Measurement Processing; Current Design and Potential Improvements," Proceedings of IEEE/ION PLANS 2008, Monterey, CA, May 2008, pp. 253-262.
- [5] Walter, T., et al., "Robust Detection of Ionospheric Irregularities," Published in *NAVIGATION*, Vol. 47, No. 2, Summer 2001, pp. 89-100, DOI 10.1002/j.2161-4296.2001.tb00231.x
- [6] COTS <http://www.militaryaerospace.com/articles/print/volume-8/issue-1/news/cots-guides-faa-toward-new-era-of-satellite-aircraft-navigation.html>.
- [7] Auld, J. and Manz, A., "The Next Generation WAAS Reference Receiver," Presented January 2005 at the Institute of Navigation (ION) National Technical Meeting, San Diego, California. pp. 544-550.

- [8] Shallberg, K. and Grabowski, J., "Considerations for Characterizing Antenna Induced Range Errors," Proceedings of the 15th International Technical Meeting of the Satellite Division of The Institute of Navigation (ION GPS 2002), Portland, OR, September 2002, pp. 809-815.
- [9] Walter, T., Enge, P., and DeCleene, B., "Integrity Lessons from the WAAS Integrity Performance Panel (WIPP)," Proceedings of the 2003 National Technical Meeting of The Institute of Navigation, Anaheim, CA, January 2003, pp. 183-194.
- [10] Gordon, S., Sherrell, C., and Potter, B.J., "WAAS Offline Monitoring," Proceedings of the 23rd International Technical Meeting of The Satellite Division of the Institute of Navigation (ION GNSS 2010), Portland, OR, September 2010, pp. 2021-2030.
- [11] Altshuler, E., Shallberg, K., Potter, B.J., and Walter, T., "Scintillation Characterization for WAAS in the Auroral Region," Proceedings of the 27th International Technical Meeting of The Satellite Division of the Institute of Navigation (ION GNSS+ 2014), Tampa, Florida, September 2014, pp. 1126-1137.
- [12] Gordon, S., Shallberg, K., Ericson, S., Grabowski, J., Morrissey, T., Lorge, F., "PRN-21 Carrier Phase Perturbations Observed by WAAS," Proceedings of the 22nd International Technical Meeting of The Satellite Division of the Institute of Navigation (ION GNSS 2009), Savannah, GA, September 2009, pp. 1236-1243.
- [13] Walter, T., Hansen, A., and Enge, P., "Message Type 28," Proceedings of the 2001 National Technical Meeting of The Institute of Navigation, Long Beach, CA, January 2001, pp. 522-532.
- [14] Blanch, J., Walter, T., Phelts, R. Eric, and Enge, P., "Near Term Improvements to WAAS Availability," Proceedings of the 2013 International Technical Meeting of The Institute of Navigation, San Diego, California, January 2013, pp. 71-77.
- [15] Blanch, J., Walter, T., Enge, P., Stern, A., and Altshuler, E., "Evaluation of a Covariance-based Clock and Ephemeris Error Bounding Algorithm for SBAS," Proceedings of the 27th International Technical Meeting of The Satellite Division of the Institute of Navigation (ION GNSS+ 2014), Tampa, Florida, September 2014, pp. 3270-3276.
- [16] Altshuler, E. S., et al., "The WAAS Ionospheric Spatial Threat Model," Proceedings of the 14th International Technical Meeting of the Satellite Division of The Institute of Navigation (ION GPS 2001), Salt Lake City, UT, September 2001, pp. 2463-2467.
- [17] Komjathy, A., Sparks, L., Mannucci, A. J., and Coster, A., "The Ionospheric Impact of the October 2003 Storm Event on WAAS," Proceedings of the 17th International Technical Meeting of the Satellite Division of The Institute of Navigation (ION GNSS 2004), Long Beach, CA, September 2004, pp. 1298-1307.
- [18] Altshuler, E., Cormier, D., and Go, H., "Improvements to the WAAS ionospheric algorithms," Proceedings of the 15th International Technical Meeting of the Satellite Division of The Institute of Navigation (ION GPS 2002), Portland, OR, September 2002, pp. 2256-2261.
- [19] Blanch, J., Walter, T., and Enge, P., "Measurement Noise versus Process Noise in Ionosphere Estimation for WAAS," Proceedings of the 2003 National Technical Meeting of The Institute of Navigation, Anaheim, CA, January 2003, pp. 854-860.
- [20] Blanch, Juan, "Using Kriging to bound Satellite Ranging Errors due to the Ionosphere," Ph.D. Dissertation, Stanford University, December 2003.

[21] Sparks, L., J. Blanch, and N. Pandya (2011), "Estimating ionospheric delay using kriging: 1. Methodology," *Radio Sci.*, 46, RS0D21, doi:10.1029/2011RS004667.

[22] Sparks, L., J. Blanch, and N. Pandya (2011), "Estimating ionospheric delay using kriging: 2. Impact on satellite-based augmentation system availability," *Radio Sci.*, 46, RS0D22, doi:10.1029/2011RS004781.

[23] Sparks, L. and Altshuler, E., "Improving WAAS Availability Along the Coast of California," Proceedings of the 27th International Technical Meeting of The Satellite Division of the Institute of Navigation (ION GNSS+ 2014), Tampa, Florida, September 2014, pp. 3299-3311.

[24] Cabler, Hank, DeCleene, Bruce, "LPV: New, Improved WAAS Instrument Approach," Proceedings of the 15th International Technical Meeting of the Satellite Division of The Institute of Navigation (ION GPS 2002), Portland, OR, September 2002, pp. 1013-1021.

[25] RTCA, DO-229E, "Minimum Operational Performance Standards for Global Positioning System/Satellite-Based Augmentation System Airborne Equipment (SBAS MOPS)," prepared by RTCA SC-159, December, 2016.

[26] Phelts, R. E., Walter, T., Enge, P., "Toward Real- Time SQM for WAAS: Improved Detection Techniques," Proceedings of the 16th International Technical Meeting of the Satellite Division of the Institute of Navigation, ION GPS/GNSS-2003, September 2003.

[27] Phelts, R. Eric, Altshuler, Eric, Walter, Todd, and Enge, Per K "Validating Nominal Bias Error Limits Using 4 years of WAAS Signal Quality Monitoring Data," Presented April 2015 at the Institute of Navigation (ION) Positioning, Navigation and Timing Conference, Honolulu, Hawaii.

[28] Shallberg, K. W., Ericson, S. D., Phelts, E., Walter, T., Kovach, K., and Altshuler, E., "Catalog and Description of GPS and WAAS L1 C/A Signal Deformation Events," Presented January 2017 at the Institute of Navigation (ION) International Technical Meeting, Monterey, California. pp. 508-520.

[29] Edgar, C., Czopek, F., Barker, B., "A Co-operative Anomaly Resolution on PRN-19," Proceedings of the 12th International Technical Meeting of the Satellite Division of The Institute of Navigation (ION GPS 1999), Nashville, TN, September 1999, pp. 2269-2268.

[30] Walter, T. and Blanch, J., "Improved User Position Monitor for WAAS," Published in *NAVIGATION*, Vol. 64, No. 1, Spring 2017, pp. 165-175, DOI 10.1002/navi.180.

[31] Bill Wanner, Bruce DeCleene, David A. Nelthropp, and Stephen Gordon, "Wide Area Augmentation System Vertical Accuracy Assessment In Support of LPV200 Requirements", *NAVIGATION*, Journal of the Institute of Navigation, Volume 55, Number 3, Fall 2008, pp. 191-203.

**Appendix
WAAS Release History)**

Date	Release	Contents
July 10, 2003 04:10 UTC	IOC	Initial WAAS Service
March 2004	CR 1	Minor performance improvements and anomaly fixes
February 10, 2005	LPV R1	Communication capacity upgrade and minor performance improvements
June 23, 2005	LPV R2	Upgrade 15 WRS to GII receivers, two thread pseudorange edit and pseudorange smoothing, remove 1 in CONUS rule from UDRE, switch from MEDLL to narrow.
January 24, 2006	LPV R3	3rd Master Station, expand IGP mask
June 23, 2006	LPV R4	Added 4 WRSs in Alaska, slope check in CNMP, dual-frequency cycle slip detection, increased AOR/POR UDRE Floors, disabled Max VTEC algorithm

August 7, 2006	LPV R4.2	Billings WRS Relocation
November 9, 2006	LPV R5.1	Added CRW as a datalink only
July 13, 2007	LPV R5.2	Added CRE with 50 m UDRE floor
July 30, 2007	LPV R5.4	Remove AOR/POR
September 27, 2007	LPV R6/7	Add 3 Mexico/2 Canada WRS, implemented Dynamic Rirreg and Extreme Storm Detector (ESD). Included 2003 & 2004 storms in undersampled threat model. Expanded IGP mask around Alaska, Mexico and East Coast. Replaced IGPS above 55 degrees north with the much denser Band 9 IGPs (131 IGPs added). CRW UDRE floor set to 50 m
March 6, 2008	LPV R8/9.1	Add 2 Mexico and 2 Canada Reference stations
September 22, 2008	LPV R8/9.2	SQM, Kriging coded (but not implemented), GIVE monitor was retuned, Unused IGPs in the pacific and furthest south of Mexico were removed from the IGP mask, new points in the northeast were added, GEO UDRE floor set to 7.5, Relative L1L2 Bias monitor
November 2009	WFO R1	CP measurement processing enhancements, misc. anomalies resolved. Added a SQM Filter Timeout Reset algorithm, change GEO unobserved bias from a static OSP to a value coming from CNMP that reduces after initial warm-up
November 11, 2010	WFO R2A	Added AMR as a data only signal
June 16, 2011	WFO R2B	Misc. anomalies resolved
October 20, 2011	WFO R3A	Fielded Kriging, AMR NPA GEO Ranging, SQM minor mod, other anomalies resolved
January 20, 2012	WFO R3A1	Removed southernmost IGPs: removed all nine IGPs at 10 degrees north latitude and the three western most IGPs at 15 degrees north latitude.
July 2012	WFO R3B	GUS switch over improvements, TJ comm node, other anomalies resolved
July 2013	WFO R4	WAAS build merge/cleanup, other anomalies resolved, changes to RDM: added median edit on clock estimate and updated phi function, UPM Kfa increased
July 2015	R43	Prep for GIII fielding, SQM Smax set to 2 to prepare for mixed GII/GIII state AMR set as data only signal via operator action (due to chronic performance issues)
August 2016	R45	SQM Smax set to 4 for GIII-only state
August 24-27, 2016	R46-CY16	Added GPS CNMP fast recovery, GEO CNMP amplitude reduction, and the Moderate Storm Detector (MSD) with Cycle 23 only supertruth V3 threat model. Increased DNU limit from 4 to 8.
October 18 2016	R47-DFO R1	Processors upgrades for WRS, GUS, O&M and Corrections Processors at C&Vs
August 16-22, 2017	R48-CY17	Chi-square UPM, reduce false maneuver detections
November 9, 2017	R48-CY17	Removed AMR
March 2018	R49-DFO R2/3	GEO5 and G-III multicast (L2C and L5 data returned from WRSs)
November 2018	R51-CY18	Minor CNMP Tuning for IIF, Minor SQM Tuning for G-III and "High C/A". Inclusion of GIVE Floor culling of the undersampled threat model + incorporation of Cycle 24 data using supertruth V5.
February 2019	R52-DFO R4	C&V Safety Processor Upgrade
September 2019	R53-DFO R5	GEO6/GUS Safety Processor Upgrade